4828 *Biochemistry* **2009,** *48,* 4828–4837
DOI: 10.1021/bi900347v

BIOCHEMISTRY
including biophysical chemistry & molecular biology
*Article*

# Augmenter of Liver Regeneration: Substrate Specificity of a Flavin-Dependent Oxidoreductase from the Mitochondrial Intermembrane Space[†]

Vidyadhar N. Daithankar, Scott R. Farrell, and Colin Thorpe*

*Department of Chemistry and Biochemistry, University of Delaware, Newark, Delaware 19716*

*Received February 28, 2009; Revised Manuscript Received April 22, 2009*

ABSTRACT: Augmenter of liver regeneration (ALR) is both a growth factor and a sulfhydryl oxidase that binds FAD in an unusual helix-rich domain containing a redox-active CxxC disulfide proximal to the flavin ring. In addition to the cytokine form of ALR (sfALR) that circulates in serum, a longer form, lfALR, is believed to participate in oxidative trapping of reduced proteins entering the mitochondrial intermembrane space (IMS). This longer form has an 80-residue N-terminal extension containing an additional, distal, CxxC motif. This work presents the first enzymological characterization of human lfALR. The N-terminal region conveys no catalytic advantage toward the oxidation of the model substrate dithiothreitol (DTT). In addition, a C71A or C74A mutation of the distal disulfide does not increase the turnover number toward DTT. Unlike Erv1p, the yeast homologue of lfALR, static spectrophotometric experiments with the human oxidase provide no evidence of communication between distal and proximal disulfides. An N-terminal His-tagged version of human Mia40, a resident oxidoreductase of the IMS and a putative physiological reductant of lfALR, was subcloned and expressed in *Escherichia coli* BL21 DE3 cells. Mia40, as isolated, shows a visible spectrum characteristic of an Fe−S center and contains 0.56 ± 0.02 atom of iron per subunit. Treatment of Mia40 with guanidine hydrochloride and triscarboxyethylphosphine hydrochloride during purification removed this chromophore. The resulting protein, with a reduced CxC motif, was a good substrate of lfALR. However, neither sfALR nor lfALR mutants lacking the distal disulfide could oxidize reduced Mia40 efficiently. Thus, catalysis involves a flow of reducing equivalents from the reduced CxC motif of Mia40 to distal and then proximal CxxC motifs of lfALR to the flavin ring and, finally, to cytochrome *c* or molecular oxygen.

Hepatic regenerative stimulator substance (*1*), now termed hepatopoietin (*2*) or augmenter of liver regeneration [ALR[1] (*3*)], was first identified as a protein that stimulated hepatocyte proliferation and liver regeneration (*1*−*4*). ALR is believed to activate the MAP kinase pathway (*5*, *6*), inhibits natural killer cells (*7*), and influences the regeneration of *Drosophila* imaginal discs (*8*). The sequence of this growth factor showed homology with two yeast proteins, Erv1p and Erv2p (*3*, *9*, *10*). All three proteins were found to be FAD-linked sulfhydryl oxidases (*11*−*14*), and the subsequent crystal structures of Erv2p (*15*) and ALR (*16*) identified a new flavin binding fold with the isoalloxazine ring inserted into the mouth of a four-helix bundle. A depiction of dimeric ALR is shown in Figure 1A. Mammalian ALR is found in two main alternatively spliced forms (*2*, *6*, *12*, *17*−*20*). The short form (sfALR, 15 kDa) is an extracellular cytokine and also participates in intracellular redox-dependent signaling pathways (*1*−*4*, *6*, *18*). The long form of the oxidase (lfALR, 23 kDa) exists predominantly in the mitochondrial intermembrane space (IMS) and contains an 80-amino acid N-terminal extension housing a second CxxC motif. The presence of additional redox-active disulfides in N- or C-terminal extensions from the core flavin binding domain is a common feature of the Erv/ALR family (*21*−*23*) where they may mediate the transfer of reducing equivalents between thiol substrate and flavin prosthetic group (see later). Figure 1B shows that these distal disulfides are placed within an N-terminal extension of lfALR and its yeast ortholog Erv1p. These regions show little sequence conservation, and in particular, the CxxC motif of lfALR is some 30 residues closer to the Erv/ALR flavin binding domain than the corresponding distal disulfide in Erv1p.

lfALR and yeast Erv1p play key roles in the generation of disulfide bonds in the mitochondrial intermembrane space (IMS) as depicted for Erv1p in Figure 2. Studies using yeast have suggested that oxidized Mia40 exchanges disulfides with a variety of proteins undergoing oxidative folding in the IMS, for example, proteins with twin $Cx_3C$ motifs (the Tim 8, 9, 10, 12, and 13

[†]This work was supported in part by National Institutes of Health Grant GM26643. The content of this work is solely the responsibility of the authors and does not necessarily reflect the official views of the National Institute of General Medical Sciences or the National Institutes of Health.

*To whom correspondence should be addressed. Phone: (302) 831-2689. Fax: (302) 831-6335. E-mail: cthorpe@udel.edu.

[1]Abbreviations: ALR, augmenter of liver regeneration (lfALR and sfALR refer to long and short forms of the protein, respectively); lfALR′, double C154A/C165A mutant of lfALR; DTNB, 5,5′-dithiobis(2-nitrobenzoate); DTT, dithiothreitol; GSH, reduced glutathione; GSSG, oxidized glutathione; IMS, mitochondrial intermembrane space; IPTG, isopropyl D-thiogalactopyranoside; QSOX, Quiescin-sulfhydryl oxidase; RNase, ribonuclease A; TCEP, triscarboxyethylphosphine hydrochloride.

 Published on Web 04/27/2009 

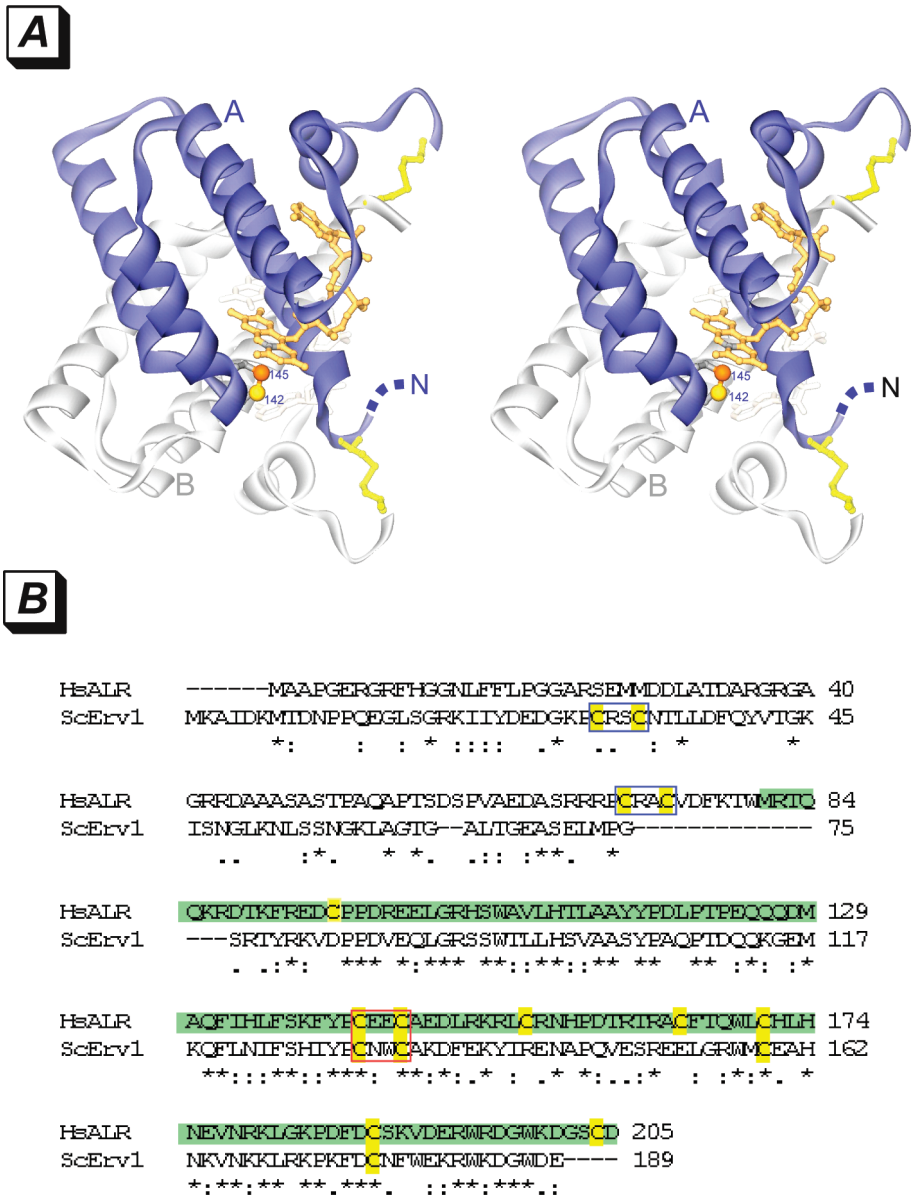


FIGURE 1: Short form of the human ALR dimer and comparison of the sequence of full-length human ALR and yeast Erv1p. (A) Homology model of the homodimer based on the structure of the short form of rat ALR (*16*, *36*). In this stereoview, the sulfur atoms of C142 and C145 of the proximal disulfide in the A subunit are shown as yellow and orange spheres, respectively. C145 is the charge-transfer donor to the isoalloxazine ring (orange in the A subunit) and will form a covalent adduct with the C4a position (colored gray in the isoalloxazine ring). The disulfides shown as yellow sticks cross-link the N- and C-termini of subunits A and B in a head-to-tail fashion. They are not required for activity of the dimer toward the model substrate DTT (*36*). (B) Comparison of the sequences of the long form of human ALR and yeast Erv1p. All cysteine residues are highlighted in yellow, and the distal and proximal disulfides are boxed in blue and red, respectively. Note the distal CxxC disulfides are placed at different positions in the N-terminal regions of Erv1p and ALR. The short form of ALR is highlighted in green.

proteins), twin $Cx_9C$ motifs (Cox17, Cox19, Mic14, Mic17, and Mdm35), the copper chaperone Ccs1, and Erv1p itself (*24*−*35*). Reduced Mia40, so generated, is then the immediate substrate of Erv1p (Figure 2).

In contrast to the yeast Erv1p/Mia40 system, rather little is known concerning possible interaction between human ALR and potential thiol substrates in the IMS. Indeed, only sfALR has been subject to a detailed enzymological investigation (*12*, *36*). This small dimeric flavoprotein (Figure 1A) is a very weak stand-alone sulfhydryl oxidase for reduced lysozyme (*12*). Dithiothreitol was later used as a convenient model substrate and exhibited $k_{cat}$ values of 50−75 $min^{-1}$ with a range of constructs of sfALR (*36*). In terms of the physiological oxidant of ALR, Farrell and Thorpe found that cytochrome *c* was a much better oxidant than molecular oxygen in vitro (*36*). They suggested that channeling reducing equivalents via the respiratory chain would avoid the generation of hydrogen peroxide associated with disulfide bond generation in the IMS (*36*). Support for this suggestion has subsequently come from in vitro and in vivo studies with yeast Erv1p (*35*, *37*). Recently, Koehler and colleagues have suggested an alternate pathway involving cytochrome *c* peroxidase-mediated oxidation of cytochrome *c* driven by the hydrogen peroxide generated by Erv1p (*38*).

This work presents the first enzymological comparison of the long and short forms of human ALR. Reductive titrations and mutagenesis are used to explore the mechanistic consequences of the inclusion of an additional distal CxxC motif within the 80-residue N-terminal extension. While the properties of full-length Erv1p (*13*, *39*) are one benchmark for our continuing studies on ALR, their distal CxxC motifs occupy different locales

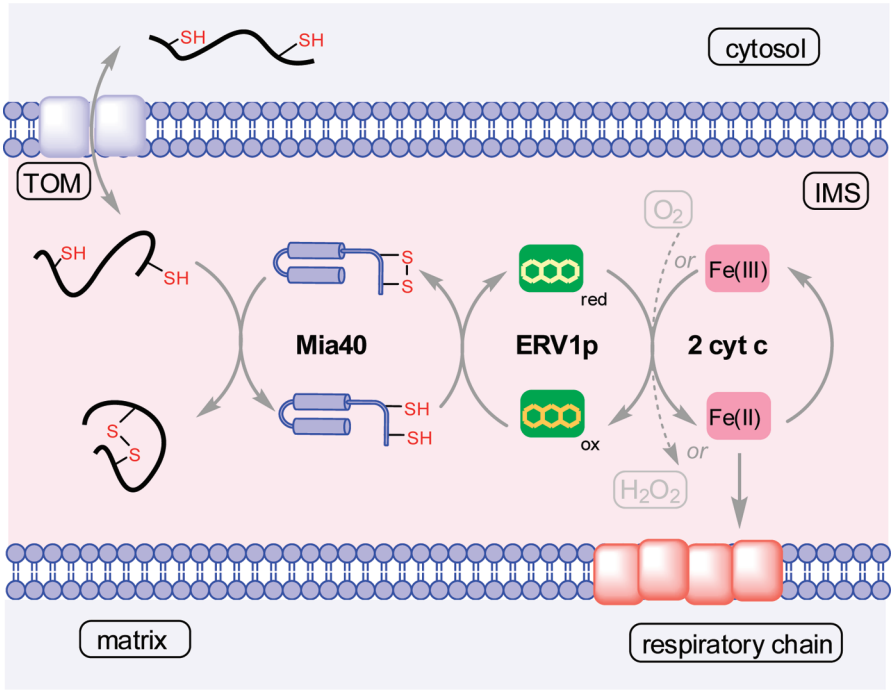


FIGURE 2: Schematic representation of the pathway for generation of disulfide bonds in the yeast mitochondrial IMS. An unfolded protein transits the outer membrane through the TOM complex and is trapped by disulfide bond generation mediated by Mia40. Regeneration of oxidized Mia40 is accomplished by Erv1p. Oxidized cytochrome *c* can serve as an oxidant of this flavoprotein, with eventual transfer of a pair of reducing equivalents to the respiratory chain for each disulfide bond generated. Alternatively, hydrogen peroxide, generated from the oxidase activity of Erv1p (gray dotted arrow), can serve as a net oxidant for cytochrome *c* peroxidase (see the text).

in divergent N-terminal regions (see Figure 1B). We further extend our studies to include the presumed physiological substrate of human lfALR, Mia40. This work suggests unanticipated new roles for Mia40 and reinforces how much more we need to know concerning oxidative protein folding and metal trafficking systems in the mitochondrial IMS.

## EXPERIMENTAL PROCEDURES

*Materials*. Ampicillin, kanamycin, chloramphenicol, tetracycline, guanidine hydrochloride, riboflavin, imidazole, urea, FAD, horse heart cytochrome *c*, GSH, GSSG, β-mercaptoethanol, bovine erythrocyte superoxide dismutase, and lysozyme were obtained from Sigma-Aldrich. Tryptone, yeast extract, NaCl, monobasic potassium phosphate, and EDTA were from Fisher Scientific. IPTG was obtained from Promega and TCEP from Pierce. DTT and DTNB were obtained from Acros Organics. Primers for mutagenesis were ordered from Integrated DNA Technologies.

*Sulfhydryl Oxidase Activity Assays*. Oxygen electrode and cytochrome *c* reductase assays were performed as described previously (*36*). Reduced RNase for discontinuous assays was prepared as described previously (*23*).

*Expression and Purification of Long Form ALR*. The clone for the long form of ALR was obtained from ATCC (IMAGE 3346679) and was then subcloned into pTrcHisA (Invitrogen) using *Nhe*I and *Hin*dIII restriction sites. PCR products were purified using the Qiagen PCR purification kit and were digested with appropriate restriction enzymes. pTrcHisA (Invitrogen) was also digested with the same restriction enzymes. DNA was purified using the Qiagen gel extraction kit and ligated using T4 DNA ligase. Ligation products were transformed into *Escherichia coli* TOP10 cells (Invitrogen) followed by sequence confirmation of the construct. The resulting plasmid was finally used to transform *E. coli* BL21 DE3 chemically competent cells (Invitrogen). Plasmids recovered from these cells were further sequenced to confirm that no additional changes had been introduced. Experimental conditions for expression and purification of lfALR were as reported previously (*36*) with the modifications mentioned here. ALR bound to the nickel-NTA column (ProBond, Invitrogen) was re-equilibrated with 10 mL of 50 mM phosphate buffer, adjusted to pH 7.5 in the presence of 6 M guanidine hydrochloride and 5 mM TCEP. Treatment with reductant and denaturant allowed for the subsequent removal of contaminants that were linked to folded lfALR via disulfide bonds. This step is not necessary with the short form of ALR (*36*). The column was then incubated for 2 h at 25 °C prior to being washed with 50 mM potassium phosphate buffer (pH 7.5) at 4 °C. The column was re-equilibrated with 100 μM FAD in the same buffer, incubated overnight, and then eluted with imidazole gradients as detailed previously (*36*).

*Removal of the N-Terminal His Tag of lfALR′ by TEV Protease*. Removal of the His tag from lfALR′ was accomplished by incubating the protein with a His-tagged TEV protease (*40*) at 30 °C for 6 h (0.1 $A_{280}$ unit of TEV protease for every 1 $A_{456}$ unit of flavoprotein) followed by passage through a Ni-NTA resin. The digested product was evaluated by SDS–PAGE to confirm removal of the N-terminal His tag.

*Human Mia40 Constructs*. A clone for human Mia40 was obtained from ATCC (IMAGE 4538841) in the pCMV-SPORT6 vector. The sequence for Mia40 was PCR amplified using the N-terminal forward primer 5′-GATGGATCCATGTCC-TATTGCCGGCAG-3′ (*Bam*HI site underlined) and the C-terminal reverse primer 5′-GGCGAATTC***TTA***ACTT-GATCCCTCCTCTTC-3′ (*Eco*RI site underlined, stop codon italicized). The PCR products were purified, using a Qiagen PCR purification kit, and digested with the restriction enzymes for 2 h at 37 °C. The pTrcHisA plasmid (Invitrogen) was also digested

with the same restriction enzymes and the linearized plasmid purified using the Qiagen gel extraction kit. Ligation with T4 DNA ligase was conducted for 3 h at room temperature. The ligated product was transformed into *E. coli* TOP10 cells (Invitrogen), and the recovered plasmid was sequenced. The plasmid was resequenced after transformation into *E. coli* BL21 DE3 and *E. coli* Rosetta-gami cells to ensure that no unanticipated mutations had been introduced.

*Mutagenesis Studies of ALR and Mia40*. The primers used for site-directed mutagenesis (QuikChange, Stratagene) are listed in the Supporting Information. Each construct was sequenced to confirm that only the desired changes were effected.

*Expression and Purification of Mia40 and Mutants*. For expression of Mia40 in *E. coli* BL21 DE3 cells, a glycerol stock was used to inoculate four 5 mL starter cultures (LB medium containing 50 $\mu$g/mL ampicillin) and grown overnight at 37 °C. The cultures were used to inoculate four 2 L flasks containing 500 mL of the same medium. At an $A_{600}$ value of approximately 0.6, the cells were induced with 1 mM IPTG and shaken for an additional 5−6 h at 37 °C. Cells were harvested by centrifugation (4000*g*, 30 min, 4 °C) and stored at −20 °C. Expression conditions were essentially the same for Rosetta-gami-DE3 cells, except that the media were additionally supplemented with kanamycin (30 $\mu$g/mL), chloramphenicol (20 $\mu$g/mL), and tetracycline (12 $\mu$g/mL). Bacterial pellets were thawed and resuspended in a total of 25 mL of 50 mM potassium phosphate buffer (pH 7.5) containing 300 mM NaCl, 0.1 mg/mL lysozyme, and one EDTA-free protease inhibitor tablet (Roche). The suspension was passed twice through a French press (at 10000 psi), followed by brief sonication to shear DNA. The cell lysate was then centrifuged at 6000*g* for 30 min. $\beta$-Mercaptoethanol (10 mM) was subsequently added to the supernatant followed by 2.5 mL of Ni-NTA resin, previously equilibrated with 50 mM potassium phosphate buffer (pH 7.5). The mixture was rocked for 1 h at 4 °C and then transferred to an empty chromatography column to allow elution of unbound material. The bound protein was then treated in two ways as detailed below.

When removal of an endogenous Fe−S chromophore (see later) was desired, the bed volume of the resin was exchanged with 50 mM potassium phosphate buffer (pH 7.5) containing 6 M guanidine hydrochloride and 5 mM TCEP, and the beads were incubated for 2 h at room temperature. The column was then transferred to the cold room and washed with 40 mL of 50 mM potassium phosphate buffer (pH 7.5) containing 10 mM $\beta$-mercaptoethanol followed by 5 mL aliquots of this solution supplemented with 50, 200, and 500 mM imidazole. Fractions were pooled after evaluation of purity by SDS−PAGE using 12% gels subsequently stained with Coomassie Brilliant Blue. Purified Mia40 was concentrated using Amicon Ultra-15 (Millipore, 10 kDa cutoff) and then desalted by applying ~0.5 mL aliquots to PD-10 columns (GE Healthcare Life Sciences) equilibrated with 50 mM potassium phosphate buffer (pH 7.5) containing 0.3 mM EDTA. Complete separation between protein thiols and $\beta$-mercaptoethanol was verified by reacting aliquots from each fraction with DTNB. Reduced protein usually emerges in fractions 5−7, and $\beta$-mercaptoethanol elutes after fraction 11. Reduced Mia40 fractions were pooled and stored under nitrogen at 4 °C. Thiol titer was rechecked using DTNB before use.

When the iron-containing form of Mia40 was being purified, the Ni-NTA-bound protein was washed with 12 mL of 50 mM phosphate buffer (pH 7.5) containing 30 mM imidazole, 300 mM NaCl, and 10 mM $\beta$-mercaptoethanol. A second wash omitted NaCl, and a third wash, additionally, omitted $\beta$-mercaptoethanol. The column was then developed with 5 mL aliquots of 50 mM phosphate buffer (pH 7.5) containing 50, 200, and 500 mM imidazole. Mia40-containing fractions were evident by their brown color and were pooled and desalted with a PD-10 column pre-equilibrated with 50 mM potassium phosphate buffer (pH 7.5).

*Anaerobic Methods, UV−Vis Spectroscopy, and Determination of Extinction Coefficients*. Anaerobic methods and cytochrome *c* assays were performed as described previously (*36*). The extinction coefficient for the flavin cofactor bound to sfALR was 11.6 $mM^{-1}$ $cm^{-1}$ at 456 nm (*36*). We obtained extinction coefficients measured in this work by recording spectra before and 1 min after the addition of 0.1% sodium dodecyl sulfate (from a 10% stock solution in water) to a solution of enzymes in 50 mM Tris buffer (pH 7.5) containing 0.3 mM EDTA. The extinction coefficient of free FAD in 0.1% detergent is 11.3 $mM^{-1}$ $cm^{-1}$ at 448 nm (*23*). The extinction coefficients used in this work were: 11.7 $mM^{-1}$ $cm^{-1}$ for lfALR′, 11.7 $mM^{-1}$ $cm^{-1}$ for C71A and C74A distal mutants, respectively, and 10.6 and 12.2 $mM^{-1}$ $cm^{-1}$ for C142A and C145A mutants of the proximal disulfide, respectively. Metal-free Mia40 concentrations were estimated using ProtParam (*41*) using an extinction coefficient of 19.9 $mM^{-1}$ $cm^{-1}$ at 280 nm. By matching the concentrations of metal-free and iron-containing Mia40 using the Bradford protein assay, we determined an extinction coefficient of 27.5 $mM^{-1}$ $cm^{-1}$ for the metalated protein.

*Metal Analysis*. Metal analysis of LB medium (16 g of tryptone, 16 g of yeast extract, 5 g of NaCl, and 2.5 g of monobasic potassium phosphate in 1 L of water adjusted to pH 7.5) and purified recombinant Mia40 was performed using a Dual View Iris Intrepid II XSP ICP spectrometer maintained at the Soil Testing Facility, Department of Plant and Soil Sciences, University of Delaware. Samples (3 mL) were mixed with 10 mL of concentrated nitric acid, sealed in XP 1500 Teflon-coated flasks, and digested for 1 min at 175 °C followed by a subsequent digestion at 180 °C for 5 min in a MARS 5 microwave oven. After cooling, the digests were brought to 50 mL with distilled deionized water, and the samples were analyzed as described above.

## RESULTS AND DISCUSSION

*Expression and Characterization of Long Form ALR*. The long form of ALR was expressed with an N-terminal hexahistidine tag for ease of purification (Figure S1 of the Supporting Information). As observed with sfALR (*36*), the presence of two nonconserved, and catalytically nonessential, cysteine residues (C154 and C165) in the long form led to the slow formation of a yellow-colored protein precipitate upon storage. Accordingly, a C154A/C165A double mutant was generated: this construct (termed lfALR′) exhibited activity comparable to that of the wild-type lfALR using DTT (entries 3 and 4 of Table 1) and remained soluble upon prolonged storage at 4 °C. Removal of the histidine tag from lfALR′ by TEV protease led to only minor changes in activity toward DTT (entry 5 of Table 1; see Experimental Procedures). Hence, the bulk of the experiments in this paper have used His-tagged constructs for ease of purification. There are small, but significant, differences in $k_{cat}/K_m$ values for the oxidation of DTT between short and long forms of ALR: the long form is ~3-fold less active [a value dominated by a 4-fold increase in the $K_m$ value (entries 2 and 4 of Table 1)]. While we do

not yet understand this effect, we later describe a more marked difference in the reactivity of short and long forms of ALR.

*Reduction of lfALR′ with Sodium Dithionite and DTT*. lfALR′ exhibited no detectable free thiols when assessed with DTNB, consistent with the expected combined presence of eight disulfides in this covalent dimer (*36*; see Experimental Procedures. Hence, the additional distal CxxC motif (C71/C74) was disulfide bridged in the oxidase as isolated. Figure 3A shows selected spectra recorded during a dithionite titration of lfALR′ under anaerobic conditions. Each subunit of lfALR′ contains three potential redox centers: the flavin cofactor, the proximal disulfide shown in Figure 1A, and the distal CxxC disulfide housed in the flexible N-terminal region (Figure 1B and Figure S1 of the Supporting Information). However, the inset of Figure 3A shows that the flavin moiety is essentially completely reduced, which is evident in the bleaching in absorbance at 456 nm, before the significant accumulation of reducing equivalents on either the proximal or distal CxxC motifs. Thus, the flavin in lfALR′ has a significantly more positive redox potential than either of these additional redox centers. As was observed for sfALR′ (*36*), reduction of lfALR′ is accompanied by the formation of significant levels of blue flavosemiquinone radical as evident by the appearance of the structured long-wavelength absorbance beyond 530 nm at the midpoint of the titration (*42*). In addition, inclusion of the 80-amino acid N-terminal extension does not change one of the most striking aspects of the reductive behavior of ALR: the generation of almost quantitative blue flavin semiquinone as oxygen is depleted during turnover with DTT ((*36*, *43*); Figure 3B).

*Behavior of Cysteine Mutants of Proximal and Distal Disulfides*. The C142A mutation of lfALR′ would leave C145 able to interact with the isoalloxazine ring [the sulfur atom of C145 is within 3.2 Å of the C4a position of the isoalloxazine ring (Figure 1A)]. This mutation does indeed generate the expected (*44*) charge-transfer complex characterized by a wedge-shaped absorption feature extending from 520 nm to beyond 700 nm (Figure 4). Subsequently, the thiolate would be expected to form a C4a flavin adduct as an intermediate in the reduction of the enzyme flavin (*44*, *45*). In contrast, the C145A mutant shows a normal yellow color devoid of significant charge-transfer absorbance (Figure 4). There is, however, a significant blue shift in the absorption maximum (from 456 to 453 nm) consistent with other proteins in which a disulfide bond proximal to a bound flavin is broken by reduction or mutagenesis (*46*−*48*). As expected for the role of a proximal disulfide in sulfhydryl oxidase catalysis, both C142 and C145 mutants of lfALR′ exhibited very low activity toward DTT (Table 1, entries 9 and 10, respectively).

In contrast, two mutants of the distal disulfide (C71A and C74A) exhibited almost the same $k_{cat}$ values with DTT and 6−8-fold lower $K_m$ values toward DTT (Table 1, entries 6 and 7, respectively). Thus, the absence of the distal disulfide (either in the context of mutation of the long form of ALR or when the N-terminal extension is totally truncated as in sfALR) leads to a several-fold decrease in $K_m$. While we do not understand the basis of these subtle effects, it is clear that DTT can access the proximal disulfide directly: the distal disulfide is not required when this nonphysiological substrate is employed.

Both C71A and C74A mutants of lfALR′ exhibit normal flavin spectra with no evidence of long wavelength bands (Figure S2A of the Supporting Information). This behavior is distinct from that of the yeast Erv1p studied by Lisowsky and colleagues (*39*). They observed that, while C33S of the distal disulfide gave a yellow enzyme, the corresponding C30S form showed an intense long wavelength charge-transfer band (*39*). The feature most reasonably reflects an internal mixed disulfide C33−C130 releasing C133 to interact with the flavin (*49*). While these data with yeast Erv1p provide strong circumstantial evidence of communication between distal and proximal disulfides, mutation of either C30 or C33 had only minor effects using DTT as a substrate of the yeast oxidase (*39*). Nevertheless, Lisowsky and colleagues report that the distal disulfide of yeast Erv1p appears to be essential in vivo (*39*).

*Additional Potential Thiol Substrates of lfALR′*. The short form of ALR was previously found to exhibit undetectable activity toward reduced glutathione (*13*). The presence of the additional distal disulfide in lfALR′ did not accelerate turnover significantly [with values of $< 1$ min$^{-1}$ using 5 mM glutathione (data not shown)]. We were further unable to detect measurable turnover of lfALR′ with unfolded reduced RNase [at 250 $\mu$M RNase thiols in 50 mM phosphate buffer (pH 7.5) (see Experimental Procedures; data not shown)]. Lisowsky and colleagues report that sfALR has very low activity toward reduced lysozyme in 2 M urea (*12*, *50*). Hence, it appears that neither short nor long forms of ALR are efficient general catalysts for the oxidation of unfolded reduced proteins in vitro.

While DTT has proved to be a very useful model substrate for several flavin-dependent sulfhydryl oxidases (*16*, *36*, *48*, *51*); its small size and marked chemical reactivity can complicate mechanistic inferences. For example, the catalytic advantage of a distal disulfide may be underestimated if DTT can reduce the proximal disulfide directly: such is the case with Erv2p and QSOX (*22*, *23*). Since Mia40 has been shown to be a substrate of yeast Erv1p (Figure 2) (*24*, *35*, *37*, *38*, *52*−*57*), we decided to test human Mia40 with short and long forms of ALR. It is important to note that there are significant differences in amino acid sequence between the yeast and human Mia40 proteins and wide variation between the N-terminal regions of yeast Erv1p and human ALR (Figure 1B). Hence, commonalities of behavior between yeast and human mitochondrial oxidative folding systems cannot be assumed without experimental verification.

*Human Mia40*. Human Mia40 is a member of the twin Cx9C protein family (*52*, *53*, *55*−*58*). The cartoon depiction (Figure 5) is based on its homology with the human Cox17 structure (*59*) and coincides adequately with a very recent NMR structure of a construct of human Mia40 (*56*). A single nonconserved cysteine residue (C4) close to the flexible N-terminus of human Mia40 is followed by a redox-active, and functionally important, CxC motif (*58*, *60*). Two structural disulfides (*58*, *60*) link the helix−turn−helix structural core of human Mia40 (Figure 5). In yeast and fungi, Mia40 has a much longer N-terminal extension that contains a transmembrane segment tethering the core domain facing the IMS (*52*, *57*, *58*, *60*). Human Mia40 lacks this transmembrane feature and could be expressed as a soluble protein in *E. coli* (*56*, *58*). An N-terminal His-tagged version of Mia40 was purified under reducing conditions and treated with guanidine hydrochloride to remove an endogenous chromophore (see later; see Experimental Procedures). The protein, as isolated, contains three thiols by DTNB titer. Since the Cx9C structural disulfide pairs of the yeast (*60*, *61*) and human (*56*) proteins are very resistant to reduction, we can assume that C4, C53, and C55 of our construct of human Mia40 are reduced as isolated (Figure 5). This reduced protein is a significant substrate of lfALR′ (Figure 6). After incubation for 30 min with 30 $\mu$M

Table 1: Steady State Kinetic Parameters for ALR Constructs Using DTT[a]

| entry | ALR construct | $k_{cat}$ (min$^{-1}$) | $K_m$ (mM) | $k_{cat}/K_m$ (M$^{-1}$ s$^{-1}$) |
|---|---|---|---|---|
| 1 | sfALR (wt)[b] | 66 ± 6 | 2.1 ± 0.5 | 520 |
| 2 | sfALR′[b] | 50 ± 3 | 2.0 ± 0.3 | 420 |
| 3 | lfALR (wt) | 88 ± 9 | 7.5 ± 1.8 | 195 |
| 4 | lfALR′ | 76 ± 5 | 8 ± 1 | 156 |
| 5 | lfALR′ (without the His tag) | 116 ± 9 | 9 ± 1 | 209 |
| 6 | lfALR′ C71A | 72 ± 2 | 0.98 ± 0.09 | 1226 |
| 7 | lfALR′ C74A | 71 ± 1 | 1.3 ± 0.7 | 944 |
| 8 | lfALR′ C71A/C74A | 108 ± 4 | 1.9 ± 0.2 | 945 |
| 9 | lfALR′ C142A | 0.25 ± 0.033[c] | nd[d] | nd[d] |
| 10 | lfALR′ C145A | 0.16 ± 0.014[c] | nd[d] | nd[d] |

[a] Turnover measurements were taken in the oxygen electrode at 25 °C in 50 mM phosphate buffer (pH 7.5) containing 0.3 mM EDTA. The constructs of ALR are detailed in the text. [b] Data from ref *36*. [c] Turnover number determined using 5 mM DTT. [d] Not determined.

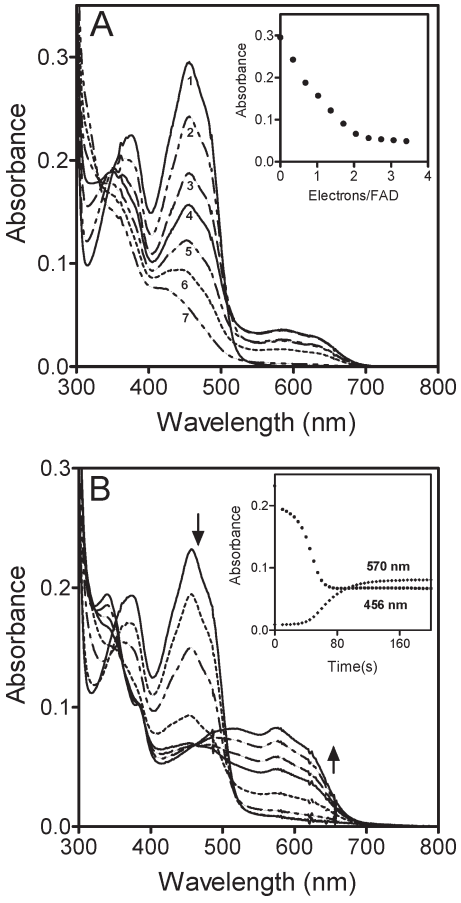


FIGURE 3: Reduction of lfALR′ by dithionite under anaerobic conditions and during aerobic turnover with DTT. (A) Curves 1−7 shows an anaerobic reduction of lfALR′ [25 μM in 50 mM phosphate buffer (pH 7.5) containing 0.3 mM EDTA] with a standardized solution of sodium dithionite (see Experimental Procedures). The inset plots the absorbance changes at 456 nm vs electron equivalents per flavin. (B) Representative spectra taken after the addition of 5 mM DTT to 20 μM lfALR′ in air-saturated buffer. The inset plots corresponding absorbance changes at 456 and 570 nm as a function of time.

reduced Mia40 (90 μM protein thiols), approximately two of three thiols have been oxidized. This is consistent with the generation of a disulfide bond between C53 and C55, while the nonconserved N-terminal cysteine residue remains reduced (Figure 5). In accord with this expectation, a C4A mutant (showing two free thiols) was oxidized by lfALR′ at a rate comparable to that shown in Figure 6 (data not shown). Hence,

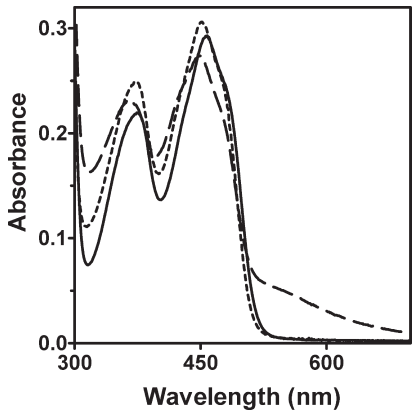


FIGURE 4: Comparison of the visible spectra of lfALR′ with proximal disulfide mutants. Spectra of 25 μM lfALR′ (—) and the corresponding C142A (− − −) and C145A (—) mutants. Extinction coefficients were determined as described in Experimental Procedures.

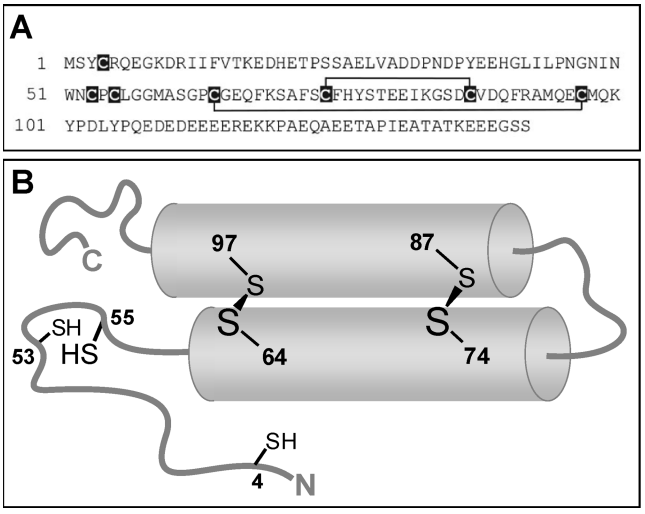


FIGURE 5: Sequence and structural cartoon of human Mia40. Panel A shows the sequence of human Mia40 with structural disulfide connectivity and cysteine residues highlighted. Panel B is a representation of the protein showing the two structural disulfides and the reduced $C_{53}XC_{55}$ motif.

this nonconserved residue is not essential for catalysis in vitro. The inset to Figure 6 plots the turnover numbers for lfALR′ as a function of the concentration of reduced wild-type Mia40 (yielding $k_{cat}$ and $K_m$ values of 13 min$^{-1}$ and 20 μM, respectively). While this turnover number appears modest, the catalytic efficiency ($k_{cat}/K_m$ of 11025 M$^{-1}$ s$^{-1}$) is some 70-fold higher than for the dithiol reductant, DTT [156 M$^{-1}$ s$^{-1}$; derived from $k_{cat}$ and $K_m$ values of 76 min$^{-1}$ and 8 mM, respectively (Table 1, entry 4)]. The His tag of the lfALR′ construct was removed using TEV protease (see Experimental Procedures) to assess its impact on the oxidation of reduced Mia40. Here, the initial rate was approximately 2-fold faster than that described above (data not shown).

Importantly, Figure 6 shows that reduced Mia40 is not a significant substrate of sfALR′ (△). In contrast, DTT is a slightly better substrate for sfALR′ than for lfALR′ (Table 1, entries 2 and 4). Further, a C71A/C74A double mutant of the distal N-terminal disulfide in lfALR′ abolished activity toward reduced Mia40 [Figure 6(●)]. Hence, the N-terminal extension of ALR, per se, does not confer reactivity to the core ALR domain toward reduced Mia40: the distal disulfide within this sequence is a critical determinant. Finally, reduced Mia40 is not a substrate of proximal disulfide mutants of lfALR′ [either C142A or C145A

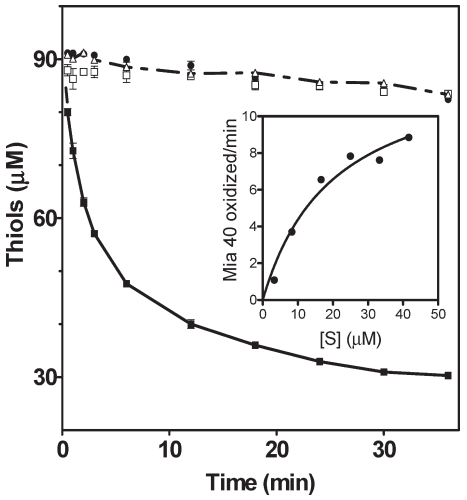


FIGURE 6: Reduced Mia40 is a substrate of lfALR′, but not of either an lfALR′ C71A/C74A double mutant or sfALR′. The main panel shows oxidation of reduced Mia40 by ALR constructs in phosphate buffer (pH 7.5) containing 0.3 mM EDTA at 25 °C, followed discontinuously using DTNB: reduced Mia40, 30 μM, alone (□); Mia40 with 1 μM lfALR′ (■); the corresponding C71A/C74A lfALR′ double mutant (●); or sfALR′ substituted for the long form (△). Data points represent the average of two separate experiments. When corrected for the nonenzymatic oxidation of Mia40 in the absence of oxidase, the initial rates were 100, 0.8, and 0.6% for lfALR′, its C71A/C74A double mutant, and sfALR′, respectively. The inset plots the concentration dependence for the initial rates of the oxidation of reduced Mia40 by 1 μM lfALR′. The curve is fit to $k_{cat}$ and $K_m$ values of 13 $min^{-1}$ and 20 μM, respectively.

(not shown)]. In sum, these data provide the first in vitro support for the role of human Mia40 as a direct substrate of human lfALR, and for the involvement of the distal disulfide in the oxidase as a mediator in the transfer of reducing equivalents from the CxC motif of Mia40 to the proximal disulfide of ALR.

*Cytochrome c as a Substrate of lfALR′*. Cytochrome *c* was initially suggested as a potential electron acceptor for ALR on the basis of experiments with the short form of this enzyme (*36*). However, lfALR is the principal ALR variant in the IMS (*34*, *62*), and hence, we determined whether it was also capable of directly reducing cytochrome *c*. Figure 7 shows that cytochrome *c* is able to serve as an effective oxidant in air-saturated solution. As observed with sfALR′, this reaction is only slightly inhibited by superoxide dismutase (Figure 7), showing that lfALR reduces the cytochrome largely directly, rather than via the intermediacy of the superoxide anion (*36*). After correction for nonenzymatic reduction of the cytochrome by reduced Mia40, the resulting initial rates show a concentration dependence that could be fitted to $k_{cat}$ and $K_m$ values of 33 $min^{-1}$ and 14 μM, respectively, for cytochrome *c*. The corresponding catalytic efficiency, $k_{cat}/K_m$, of $3.9 \times 10^4$ $M^{-1}$ $s^{-1}$ toward cytochrome *c* is some 12-fold lower than that obtained using sfALR′ (270 $min^{-1}$, 10 μM; $4.5 \times 10^5$ $M^{-1}$ $s^{-1}$) measured with DTT as the reducing substrate (*36*). Several factors might impact this decreased catalytic efficiency. For example, the 80-residue N-terminal extension in lfALR may partially impede the approach of cytochrome *c*. In addition, the 80 N-terminal residues (calculated pI of 8.9; see Table S1 of the Supporting Information) might confer some measure of electrostatic repulsion to the highly basic cytochrome [pI of ~10 (*63*)] at pH 7.5. In contrast, the positive charge of the N-terminal region of lfALR might favor the approach of the negatively charged human Mia40 [pI 4.2 (Table S1 of the Supporting Information)].

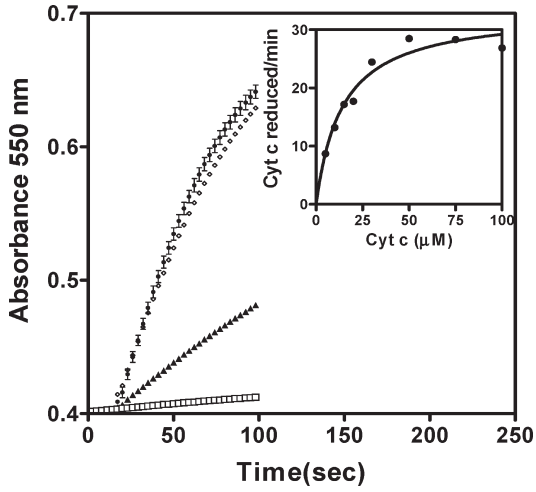


FIGURE 7: lfALR catalyzes the reduction of cytochrome *c* by reduced Mia40. The main panel shows the absorbance of 30 μM cytochrome *c* at 25 °C in 50 mM phosphate buffer (pH 7.5) containing 0.3 mM EDTA (□), with the addition of 50 μM reduced Mia40 (▲), and then with the further addition at 20 s of 1 μM lfALR′ (●, duplicates) or with ALR and 25 μg/mL superoxide dismutase (◇, duplicates). The inset shows turnover numbers for cytochrome *c* reduction fit to the Michaelis−Menten equation.

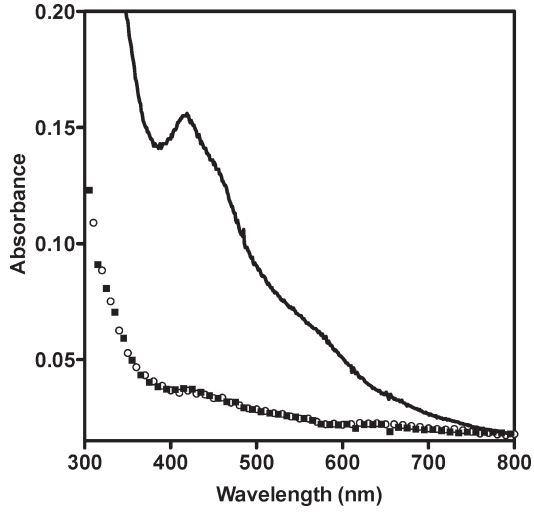


FIGURE 8: UV−vis spectrum of human Mia40 samples prepared in this work. The solid line shows the spectrum of 50 μM Mia40 in 50 mM phosphate buffer (pH 7.5). The protein was purified from *E. coli* BL21 DE3 cells in the absence of denaturant (see Experimental Procedures). The spectrum of 50 μM Mia40 isolated from Rosetta-gami DE3 cells is shown with black squares. White circles correspond to 50 μM protein purified from BL21 cells in the presence of denaturant and reductant (see Experimental Procedures). No precautions were taken to exclude oxygen from buffers during purification of these proteins.

*An Unanticipated Role of Mia40 in Iron Binding?*. Previously, Cox17, a twin Cx9C protein, has been shown to bind copper via its N-terminal CC motif (*59*, *64*, *65*). Further, Terziyska et al. have demonstrated that yeast Mia40 binds both copper and zinc and have suggested that this interaction is functionally important (*52*). This study used a maltose binding protein fusion construct of yeast Mia40 expressed in *E. coli* cells that were grown in medium supplemented with either cupric sulfate or zinc acetate at 100 μM (*52*). When we purified human MIA40 in the presence of β-mercaptoethanol, but in the absence of denaturant (see Experimental Procedures), the protein always exhibited a distinct brown color with a visible

spectrum suggestive of an iron−sulfur cluster (Figure 8). The chromophore was bleached in air-saturated phosphate buffer (pH 7.5) with a half-time of approximately 2 weeks at 4 °C using 130 $\mu$M Mia40 (data not shown). Inductively coupled plasma spectrometry (see Experimental Procedures) of three independent preparations showed 0.56 ± 0.02 atom of iron compared to 0.010 ± 0.003 and 0.065 ± 0.012 atom of copper and zinc, respectively (see Figure S3 of the Supporting Information). These data were obtained with standard LB growth medium unsupplemented with additional metals. Analysis of the media used for these experiments showed metal contents (15 $\mu$M Fe, 28 $\mu$M Zn, and 0.5 $\mu$M Cu) that were considerably lower than the 100 $\mu$M supplements of zinc and copper used previously (*52*).

Since we have previously expressed other disulfide-containing proteins in *E. coli* Rosetta-gami DE3 cells (*23*), a strain with a cytosol more oxidizing than that of normal *E. coli* cells, we investigated their utility in the expression of Mia40 (see Experimental Procedures). The resulting protein exhibited a thiol titer of 0.90 ± 0.18, consistent with a disulfide at the CxC motif with the nonconserved C4 as a free thiol. Since metal binding would likely involve the reduced CxC motif (see above), the oxidized protein would be expected to contain little or no iron. In accord with this expectation, oxidized Mia40 exhibited little absorbance in the visible region (Figure 8) and an iron content of 0.053 atom/subunit (Figure S3 of the Supporting Information). The recent NMR structure of human Mia40 published by Banci et al. also utilized *E. coli* Origami cells to obtain oxidized protein, and it is thus not surprising that their preparations did not contain appreciable iron: their structure shows a CxC disulfide in the N-terminal region of the protein.

We recognize that considerable caution needs to be exercised when inferences are drawn from the metal content of eukaryotic proteins that have been expressed heterologously in bacteria (*66*). For example, the metal homeostasis mechanisms, including the metal chaperone systems and the intracellular concentrations of metal ions, may differ profoundly between organisms and hence confound conclusions of physiological relevance (*66*−*69*). However, our results are of interest because Lill and co-workers have reported that yeast expressing a temperature-sensitive mutant of Erv1p were unable to assemble cytosolic Fe−S centers at nonpermissive temperatures (*34*, *67*). They further demonstrated that lfALR and Erv1p were functional orthologs in Fe−S center trafficking across the IMS (*34*). We examined whether an Fe−S center could be incorporated into human lfALR′ [exploiting the usual methods of incubation with ferrous ammonium sulfate, sodium sulfide, and $\beta$-mercaptoethanol under anaerobic conditions (*70*−*72*)]. These exploratory experiments were unconvincing (data not shown). Correspondingly, Lange et al. found no stable association of an Fe−S cluster with yeast Erv1p even under anaerobic conditions (*34*). Our present finding that Mia40 binds iron strongly in vitro suggests an alternative hypothesis, that Mia40 may participate in an Fe−S delivery system that is enabled, directly or indirectly, by Erv1p in yeast or by lfALR in human mitochondria.

*Conclusions*. This contribution shows that the reduced CxC motif in human Mia40 transfers reducing equivalents to the mitochondrial form of ALR, but not to the shorter variant that functions as a circulating growth factor. The reaction is obligatorily dependent on the distal CxxC found in the N-terminal extension of lfALR. While communication between distal and proximal disulfide/dithiol redox centers in lfALR is not evident from static titrations, it proves functionally important in the oxidation of reduced Mia40. In addition to the roles of Mia40 in the oxidative trapping of small proteins within the IMS, our data suggest that Mia40 may also play a direct role in Fe−S traffic in the IMS.

## ACKNOWLEDGMENT

We thank Drs. Deborah Fass and David Waugh for a plasmid expressing TEV protease, Cathy Olsen for generous help with metal analyses, and Mr. Vamsi Kodali for insightful comments on the manuscript.

## SUPPORTING INFORMATION AVAILABLE

Table S1, Figures S1−S3, and a listing of primers used for site-directed mutagenesis provide supplementary data, sequences, and analysis for human Mia40 and lfALR′. This material is available free of charge via the Internet at http://pubs.acs.org.

## REFERENCES

1. LaBrecque, D. R., and Pesch, L. A. (1975) Preparation and partial characterization of hepatic regenerative stimulator substance (SS) from rat liver. *J. Physiol. 248*, 273–284.
2. Chen, X., Li, Y., Wei, K., Li, L., Liu, W., Zhu, Y., Qiu, Z., and He, F. (2003) The potentiation role of hepatopoietin on activator protein-1 is dependent on its sulfhydryl oxidase activity. *J. Biol. Chem. 278*, 49022–49030.
3. Hagiya, M., Francavilla, A., Polimeno, L., Ihara, I., Sakai, H., Seki, T., Shimonishi, M., Porter, K. A., and Starzl, T. E. (1994) Cloning and sequence analysis of the rat augmenter of liver regeneration (ALR) gene: Expression of biologically active recombinant ALR and demonstration of tissue distribution. *Proc. Natl. Acad. Sci. U.S.A. 91*, 8142–8146.
4. Zhang, L. M., Liu, D. W., Liu, J. B., Zhang, X. L., Wang, X. B., Tang, L. M., and Wang, L. Q. (2005) Effect of naked eukaryotic expression plasmid encoding rat augmenter of liver regeneration on acute hepatic injury and hepatic failure in rats. *World J. Gastroenterol. 11*, 3680–3685.
5. Li, Y., Li, M., Xing, G., Hu, Z., Wang, Q., Dong, C., Wei, H., Fan, G., Chen, J., Yang, X., Zhao, S., Chen, H., Guan, K., Wu, C., Zhang, C., and He, F. (2000) Stimulation of the mitogen-activated protein kinase cascade and tyrosine phosphorylation of the epidermal growth factor receptor by hepatopoietin. *J. Biol. Chem. 275*, 37443–37447.
6. Pawlowski, R., and Jura, J. (2006) ALR and Liver Regeneration. *Mol. Cell. Biochem. 288*, 159–169.
7. Tanigawa, K., Sakaida, I., Masuhara, M., Hagiya, M., and Okita, K. (2000) Augmenter of liver regeneration (ALR) may promote liver regeneration by reducing natural killer (NK) cell activity in human liver diseases. *J. Gastroenterol. 35*, 112–119.
8. McClure, K. D., Sustar, A., and Schubiger, G. (2008) Three genes control the timing, the site and the size of blastema formation in *Drosophila*. *Dev. Biol. 319*, 68–77.
9. Lisowsky, T. (1992) Dual function of a new nuclear gene for oxidative phosphorylation and vegetative growth in yeast. *Mol. Gen. Genet. 232*, 58–64.
10. Stein, G., and Lisowsky, T. (1998) Functional comparison of the yeast scERV1 and scERV2 genes. *Yeast 14*, 171–180.
11. Gerber, J., Muhlenhoff, U., Hofhaus, G., Lill, R., and Lisowsky, T. (2001) Yeast ERV2p is the first microsomal FAD-linked sulfhydryl oxidase of the Erv1p/Alrp protein family. *J. Biol. Chem. 276*, 23486–23491.
12. Lisowsky, T., Lee, J. E., Polimeno, L., Francavilla, A., and Hofhaus, G. (2001) Mammalian augmenter of liver regeneration protein is a sulfhydryl oxidase. *Dig. Liver Dis. 33*, 173–180.
13. Lee, J., Hofhaus, G., and Lisowsky, T. (2000) Erv1p from *Saccharomyces cerevisiae* is a FAD-linked sulfhydryl oxidase. *FEBS Lett. 477* (1−2), 62–66.
14. Sevier, C. S., Cuozzo, J. W., Vala, A., Aslund, F., and Kaiser, C. A. (2001) A flavoprotein oxidase defines a new endoplasmic reticulum pathway for biosynthetic disulphide bond formation. *Nat. Cell Biol. 3*, 874–882.
15. Gross, E., Sevier, C. S., Vala, A., Kaiser, C. A., and Fass, D. (2002) A new FAD-binding fold and intersubunit disulfide shuttle in the thiol oxidase Erv2p. *Nat. Struct. Biol. 9*, 61–67.
16. Wu, C. K., Dailey, T. A., Dailey, H. A., Wang, B. C., and Rose, J. P. (2003) The crystal structure of augmenter of liver regeneration:

A mammalian FAD-dependent sulfhydryl oxidase. *Protein Sci. 12*, 1109–1118.
17. Li, Y., Wei, K., Lu, C., Li, M., Xing, G., Wei, H., Wang, Q., Chen, J., Wu, C., Chen, H., Yang, S., and He, F. (2002) Identification of hepatopoietin dimerization, its interacting regions and alternative splicing of its transcription. *Eur. J. Biochem. 269*, 3888–3893.
18. Gatzidou, E., Kouraklis, G., and Theocharis, S. (2006) Insights on augmenter of liver regeneration cloning and function. *World J. Gastroenterol. 12*, 4951–4958.
19. Francavilla, A., Hagiya, M., Porter, K. A., Polimeno, L., Ihara, I., and Starzl, T. E. (1994) Augmenter of liver regeneration: Its place in the universe of hepatic growth factors. *Hepatology 20*, 747–757.
20. Polimeno, L., Lisowsky, T., and Francavilla, A. (1999) From yeast to man: From mitochondria to liver regeneration: A new essential gene family. *Ital. J. Gastroenterol. Hepatol. 31*, 494–500.
21. Vitu, E., Bentzur, M., Lisowsky, T., Kaiser, C. A., and Fass, D. (2006) Gain of function in an ERV/ALR sulfhydryl oxidase by molecular engineering of the shuttle disulfide. *J. Mol. Biol. 362*, 89–101.
22. Fass, D. (2008) The Erv family of sulfhydryl oxidases. *Biochim. Biophys. Acta 1783*, 557–566.
23. Heckler, E. J., Alon, A., Fass, D., and Thorpe, C. (2008) Human quiescin-sulfhydryl oxidase, QSOX1: Probing internal redox steps by mutagenesis. *Biochemistry 47*, 4955–4963.
24. Mesecke, N., Terziyska, N., Kozany, C., Baumann, F., Neupert, W., Hell, K., and Herrmann, J. M. (2005) A disulfide relay system in the intermembrane space of mitochondria that mediates protein import. *Cell 121*, 1059–1069.
25. Terziyska, N., Grumbt, B., Bien, M., Neupert, W., Herrmann, J. M., and Hell, K. (2007) The sulfhydryl oxidase Erv1 is a substrate of the Mia40-dependent protein translocation pathway. *FEBS Lett. 581*, 1098–1102.
26. Gabriel, K., Milenkovic, D., Chacinska, A., Muller, J., Guiard, B., Pfanner, N., and Meisinger, C. (2007) Novel mitochondrial intermembrane space proteins as substrates of the MIA import pathway. *J. Mol. Biol. 365*, 612–620.
27. Hell, K. (2008) The Erv1-Mia40 disulfide relay system in the intermembrane space of mitochondria. *Biochim. Biophys. Acta 1783*, 601–609.
28. Herrmann, J. M., and Kohl, R. (2007) Catch me if you can! Oxidative protein trapping in the intermembrane space of mitochondria. *J. Cell Biol. 176*, 559–563.
29. Koehler, C. M., and Tienson, H. L. (2009) Redox regulation of protein folding in the mitochondrial intermembrane space. *Biochim. Biophys. Acta 1793*, 139–145.
30. Stojanovski, D., Milenkovic, D., Muller, J. M., Gabriel, K., Schulze-Specking, A., Baker, M. J., Ryan, M. T., Guiard, B., Pfanner, N., and Chacinska, A. (2008) Mitochondrial protein import: Precursor oxidation in a ternary complex with disulfide carrier and sulfhydryl oxidase. *J. Cell Biol. 183*, 195–202.
31. Tokatlidis, K. (2005) A disulfide relay system in mitochondria. *Cell 121*, 965–967.
32. Reddehase, S., Grumbt, B., Neupert, W., and Hell, K. (2009) The Disulfide Relay System of Mitochondria Is Required for the Biogenesis of Mitochondrial Ccs1 and Sod1. *J. Mol. Biol. 385*, 331–338.
33. Kawamata, H., and Manfredi, G. (2008) Different regulation of wild-type and mutant Cu,Zn superoxide dismutase localization in mammalian mitochondria. *Hum. Mol. Genet. 17*, 3303–3317.
34. Lange, H., Lisowsky, T., Gerber, J., Muhlenhoff, U., Kispal, G., and Lill, R. (2001) An essential function of the mitochondrial sulfhydryl oxidase Erv1p/ALR in the maturation of cytosolic Fe/S proteins. *EMBO Rep. 2*, 715–720.
35. Allen, S., Balabanidou, V., Sideris, D. P., Lisowsky, T., and Tokatlidis, K. (2005) Erv1 Mediates the Mia40-dependent Protein Import Pathway and Provides a Functional Link to the Respiratory Chain by Shuttling Electrons to Cytochrome c. *J. Mol. Biol. 353*, 937–944.
36. Farrell, S. R., and Thorpe, C. (2005) Augmenter of liver regeneration: A flavin dependent sulfhydryl oxidase with cytochrome C reductase activity. *Biochemistry 44*, 1532–1541.
37. Bihlmaier, K., Mesecke, N., Terziyska, N., Bien, M., Hell, K., and Herrmann, J. M. (2007) The disulfide relay system of mitochondria is connected to the respiratory chain. *J. Cell Biol. 179*, 389–395.
38. Dabir, D. V., Leverich, E. P., Kim, S. K., Tsai, F. D., Hirasawa, M., Knaff, D. B., and Koehler, C. M. (2007) A role for cytochrome c and cytochrome c peroxidase in electron shuttling from Erv1. *EMBO J. 26*, 4801–4811.
39. Hofhaus, G., Lee, J. E., Tews, I., Rosenberg, B., and Lisowsky, T. (2003) The N-terminal cysteine pair of yeast sulfhydryl oxidase Erv1p is essential for in vivo activity and interacts with the primary redox centre. *Eur. J. Biochem. 270*, 1528–1535.
40. Tropea, J. E., Cherry, S., and Waugh, D. S. (2009) Expression and purification of soluble His(6)-tagged TEV protease. *Methods Mol. Biol. 498*, 297–307.
41. Gasteiger, E., Gattiker, A., Hoogland, C., Ivanyi, I., Appel, R. D., and Bairoch, A. (2003) ExPASy: The proteomics server for in-depth protein knowledge and analysis. *Nucleic Acids Res. 31*, 3784–3788.
42. Massey, V. (2000) The chemical and biological versatility of riboflavin. *Biochem. Soc. Trans. 28*, 283–296.
43. Kay, C. W. M., Elsasser, C., Bittl, R., Farrell, S. R., and Thorpe, C. (2006) Determination of the distance between the two neutral flavin radicals in augmenter of liver regeneration by pulsed ELDOR. *J. Am. Chem. Soc. 128*, 76–77.
44. Williams, C. H., Jr. (1992) in *Chemistry and Biochemistry of Flavoenzymes* (Muller, F., Ed.) pp 121−211, CRC Press, Boca Raton, FL.
45. Thorpe, C., and Williams, C. H. (1976) Spectral evidence for a flavin adduct in a monoalkylated derivative of pig heart lipoamide dehydrogenase. *J. Biol. Chem. 251*, 7726–7728.
46. Thorpe, C., and Williams, C. H. (1976) Differential reactivity of the two active site cysteine residues generated on reduction of pig heart lipoamide dehydrogenase. *J. Biol. Chem. 251*, 3553–3557.
47. Brohawn, S. G., Rudik, I., and Thorpe, C. (2003) Avian sulfhydryl oxidase is not a metalloenzyme: Adventitious binding of divalent metal ions to the enzyme. *Biochemistry 42*, 11074–11082.
48. Wang, W., Winther, J. R., and Thorpe, C. (2007) Erv2p: Characterization of the redox behavior of a yeast sulfhydryl oxidase. *Biochemistry 46*, 3246–3254.
49. Coppock, D. L., and Thorpe, C. (2006) Multidomain flavin-dependent sulfhydryl oxidases. *Antioxid. Redox Signaling 8*, 300–311.
50. Hofhaus, G., and Lisowsky, T. (2002) Sulfhydryl oxidases as factors for mitochondrial biogenesis. *Methods Enzymol. 348*, 314–324.
51. Rodriguez, I., Redrejo-Rodriguez, M., Rodriguez, J. M., Alejo, A., Salas, J., and Salas, M. L. (2006) African swine fever virus pB119L protein is a flavin adenine dinucleotide-linked sulfhydryl oxidase. *J. Virol. 80*, 3157–3166.
52. Terziyska, N., Lutz, T., Kozany, C., Mokranjac, D., Mesecke, N., Neupert, W., Herrmann, J. M., and Hell, K. (2005) Mia40, a novel factor for protein import into the intermembrane space of mitochondria is able to bind metal ions. *FEBS Lett. 579*, 179–184.
53. Chacinska, A., Pfannschmidt, S., Wiedemann, N., Kozjak, V., Sanjuan Szklarz, L. K., Schulze-Specking, A., Truscott, K. N., Guiard, B., Meisinger, C., and Pfanner, N. (2004) Essential role of Mia40 in import and assembly of mitochondrial intermembrane space proteins. *EMBO J. 23*, 3735–3746.
54. Chacinska, A., Lind, M., Frazier, A. E., Dudek, J., Meisinger, C., Geissler, A., Sickmann, A., Meyer, H. E., Truscott, K. N., Guiard, B., Pfanner, N., and Rehling, P. (2005) Mitochondrial presequence translocase: Switching between TOM tethering and motor recruitment involves Tim21 and Tim17. *Cell 120*, 817–829.
55. Stojanovski, D., Muller, J. M., Milenkovic, D., Guiard, B., Pfanner, N., and Chacinska, A. (2008) The MIA system for protein import into the mitochondrial intermembrane space. *Biochim. Biophys. Acta 1783*, 610–617.
56. Banci, L., Bertini, I., Cefaro, C., Ciofi-Baffoni, S., Gallo, A., Martinelli, M., Sideris, D. P., Katrakili, N., and Tokatlidis, K. (2009) MIA40 is an oxidoreductase that catalyzes oxidative protein folding in mitochondria. *Nat. Struct. Mol. Biol. 16*, 198–206.
57. Naoe, M., Ohwa, Y., Ishikawa, D., Ohshima, C., Nishikawa, S., Yamamoto, H., and Endo, T. (2004) Identification of Tim40 that mediates protein sorting to the mitochondrial intermembrane space. *J. Biol. Chem. 279*, 47815–47821.
58. Hofmann, S., Rothbauer, U., Muhlenbein, N., Baiker, K., Hell, K., and Bauer, M. F. (2005) Functional and mutational characterization of human MIA40 acting during import into the mitochondrial intermembrane space. *J. Mol. Biol. 353*, 517–528.
59. Banci, L., Bertini, I., Ciofi-Baffoni, S., Janicka, A., Martinelli, M., Kozlowski, H., and Palumaa, P. (2007) A structural-dynamical characterization of human Cox17. *J. Biol. Chem. 283*, 7912–7920.
60. Grumbt, B., Stroobant, V., Terziyska, N., Israel, L., and Hell, K. (2007) Functional characterization of Mia40p, the central component of the disulfide relay system of the mitochondrial intermembrane space. *J. Biol. Chem. 282*, 37461–37470.
61. Terziyska, N., Grumbt, B., Kozany, C., and Hell, K. (2009) Structural and functional roles of the conserved cysteine residues of the redox-regulated import receptor Mia40 in the intermembrane space of mitochondria. *J. Biol. Chem. 284*, 1353–1363.
62. Klissenbauer, M., Winters, S., Heinlein, U. A., and Lisowsky, T. (2002) Accumulation of the mitochondrial form of the sulphydryl oxidase Erv1p/Alrp during the early stages of spermatogenesis. *J. Exp. Biol. 205*, 1979–1986.

63. Barlow, G. H., and Margoliash, E. (1966) Electrophoretic behavior of mammalian-type cytochromes c. *J. Biol. Chem. 241*, 1473–1477.
64. Beers, J., Glerum, D. M., and Tzagoloff, A. (1997) Purification, characterization, and localization of yeast Cox17p, a mitochondrial copper shuttle. *J. Biol. Chem. 272*, 33191–33196.
65. Heaton, D. N., George, G. N., Garrison, G., and Winge, D. R. (2001) The mitochondrial copper metallochaperone Cox17 exists as an oligomeric, polycopper complex. *Biochemistry 40*, 743–751.
66. Maret, W. (2008) Zinc Proteomics and the Annotation of the Human Zinc Proteome. *Pure Appl. Chem. 20*, 2679–2687.
67. Lill, R., and Muhlenhoff, U. (2008) Maturation of iron-sulfur proteins in eukaryotes: Mechanisms, connected processes, and diseases. *Annu. Rev. Biochem. 77*, 669–700.
68. Ramelot, T. A., Cort, J. R., Goldsmith-Fischman, S., Kornhaber, G. J., Xiao, R., Shastry, R., Acton, T. B., Honig, B., Montelione, G. T., and Kennedy, M. A. (2004) Solution NMR structure of the iron-sulfur cluster assembly protein U (IscU) with zinc bound at the active site. *J. Mol. Biol. 344*, 567–583.
69. Liu, J., Oganesyan, N., Shin, D. H., Jancarik, J., Yokota, H., Kim, R., and Kim, S. H. (2005) Structural characterization of an iron-sulfur cluster assembly protein IscU in a zinc-bound form. *Proteins 59*, 875–881.
70. Rabinowitz, J. (1972) Preparation and properties of clostridial ferredoxins. *Methods Enzymol. 24*, 431–446.
71. Kulzer, R., Pils, T., Kappl, R., Huttermann, J., and Knappe, J. (1998) Reconstitution and characterization of the polynuclear iron-sulfur cluster in pyruvate formate-lyase-activating enzyme. Molecular properties of the holoenzyme form. *J. Biol. Chem. 273*, 4897–4903.
72. Johnson, M. K. (1998) Iron-sulfur proteins: New roles for old clusters. *Curr. Opin. Chem. Biol. 2*, 173–181.